ISSN 1392 - 1207. MECHANIKA. 2013 Volume 19(1): 96-103

Welding of a 7025 Al-alloy by a pulsed MIG welding process

P. Kah*, M. Olabode, E. Hiltunen***, J. Martikainen******

**Lappeenranta University of Technology, Lappeenranta, Finland, E-mail: paul.kah@lut.fi*
***Lappeenranta University of Technology, Lappeenranta, Finland, E-mail: muyiwa.olabode@lut.fi*
****Lappeenranta University of Technology, Lappeenranta, Finland, E-mail: esa.hiltunen@lut.fi*
*****Lappeenranta University of Technology, Lappeenranta, Finland, E-mail: jukka.martikainen@lut.fi*

crossref http://dx.doi.org/10.5755/j01.mech.19.1.3618

1. Introduction

Aluminium has advantageous mechanical, chemical, electrical and thermal properties that make it very important in structural engineering. It has found wide application in the transportation industry, particularly the automobile and airline industry, due to its low weight-to-strength ratio. The prospects of aluminium becoming a predominant material in automobile manufacture are becoming evident. A major challenge facing construction with aluminium is the additional cost of manufacturing aluminium structures resulting from the extra care needed when welding aluminium.

Aluminium alloys are categorised based on the manufacturing process and alloy composition. The two main classes of aluminium alloys are cast aluminium alloys and wrought aluminium alloys. Each class is divided into series based on the major alloying element in the alloy. For the most commonly found applications the more interesting group is wrought aluminium alloys as they possess higher strength than cast aluminium alloys. Any aluminium alloy 7XXX is a member of the class of wrought aluminium alloys [1].

This study analyses the effect of heat input in the pulsed metal inert gas (MIG) welding of a 7025 Al-alloy of 5 mm thickness. The effect of varying the welding speed is researched. The metallurgy of the 7025 Al-alloy is studied in the fusion zone, partially melted zone and the heat affected zone. Results are presented as micrograph, macrographs and hardness graphs. The experiments and tests were made in accordance with SFS standards and quality assurance was done based on EN 1090-3.

2. Weldability

The weldability of aluminium alloys using traditional fusion processes is sometimes problematic. While the vast majority of alloys (1XXX, 3XXX, 4XXX, 5XXX and 6XXX alloys) have reasonable to optimal weldability, others can have metallurgical drawbacks, such as embrittlement (2XXX and 7XXX). Recently, the weldability of the 7XXX has been re-evaluated since the use of solid-state metal welding processes (FSW) mitigates some of the undesired effects [2]. Several important factors influence the weldability of aluminium and its alloys, some of which apply to all aluminium alloys and some to individual alloy series. The main factors to be considered in detail when welding aluminium are [3]:

- the presence of a tenacious, refractory surface oxide film which can cause lack of fusion or porosity, if not removed before welding;
- the high solubility of hydrogen in liquid aluminium compared with its solubility in solid aluminium, which can lead to porosity in weld metal;
- the tendency for some alloys, notably 2XXX, 6XXX and 7XXX series alloys, to suffer hot cracking or heat affected zone (HAZ) liquation cracking;
- the reduction in mechanical properties that occurs across the weld zone when aluminium alloys are welded.

3. Experimental setup and procedures

This section describes hardness testing and macroscopic examination, and also presents the material specimen, joint preparation process and experiment parameters and consumables. Analysis of the 7025 alloy and the quality of the welds is also presented.

3.1. Materials

The base material specimen used was a 7025-T6 plate of 5 mm thickness. The chemical composition of the material is presented in Table 1. Wire brushing was used to clean the oxide layer from the workpiece before welding. The time interval between cleaning and welding was less than two minutes. Care was taken to ensure no contamination before the welding. Joint surface cleaning is important to remove the thin oxide layer of aluminium (Al_2O_3) found on aluminium surfaces. The Al_2O_3 layer regenerates itself when scratched and is responsible for the corrosion resistance of aluminium alloys [3]. In welding it is responsible for arc instability problems because it is electrically non-conductive. Al_2O_3 is hygroscopic and is usually found in hydrated form. The melting temperature of Al_2O_3 is 2060°C which is high compared to the melting temperature range of 7XXX alloys, 476 - 657°C [4, 5]. The welding wire used in the experiment was 4043 aluminium filler wire with chemical composition as presented in Table 1. Typical mechanical properties of the wire include: yield stress of 55 MPa, tensile strength of 165 MPa, and an elongation of 18%. The shielding gas was 99.995% Ar, which was supplied through the MIG torch to protect the weld pool from the atmosphere. This approach was chosen since heated metal (around the melting point) usually exhibits a tendency to react with the atmosphere to form oxides and nitrides. Argon is the recommended shielding gas for welding 7XXX aluminium using pulsed MIG [6].

Table 1

Chemical composition of 7025 (workpiece) and 4043 (filler wire) aluminium alloys (wt%)

Elements	Al (%)	Be (%)	Cr (%)	Cu (%)	Fe (%)	Mg (%)	Mn (%)	Si (%)	Ti (%)	Zn (%)	Other, each (%)	Other, total (%)
7025	91.5	-	0.30	0.10	0.40	1.50	0.60	0.30	0.10	5.0	0.050	0.15
ER 4043	-	0.0001	-	0.01	0.2	0.01	0.01	4.8	0.02	0.01	-	-

3.2. Welding equipment

Pulsed MIG welding was chosen since it is suitable for all joint types in out-of-position welding of 1.0 - 6.0 mm plate thicknesses. In many cases AC - TIG welding can also be used. Pulsed MIG is suitable when high quality is required and when productivity and economics are important elements [6].

The equipment used in this experiment included a robot workstation and the arc power source used in the experiment was a cold metal transfer (CMT) power source from Fronius. The Fronius TPS 4000 CMT power source (max 400 A 50%) has the required synergy property to get a pulse parameter; the current value and other parameters change automatically. The MIG torch used was a Fronius Robacta 5000 36^{o} (max 500 A) (manufactured by Fronius International). The torch was connected to a Motorman (EA1900N) robot. Fig. 1 shows a schematic setup of the experiment. The robot has 6 axes and can attain an accuracy of up to +/- 0.06 mm. The welding torch was inclined at 10° pushing to the workpiece and the workpiece was clamped to the workbench with a vice. The workbench could be rotated in a clockwise and anticlockwise direction thereby allowing for more flexibility in changing workpiece orientation. In addition, the robot base is able to slide along the rail on its base, which makes the workstation area quite large. The power source (CMT) supplies the filler wire which is passed through the torch to the weld pool. The gas passes through piping attached to the robot and then to the torch. The filler wire extension was 2 mm and the nozzle to work distance (stickout length) was 15 mm. The workstation is caged during automated welding operations and the pulses are generated and controlled by the arc power source. Pulse analysis (obtained via an oscilloscope) was done to obtain the pulse frequency. The pulse current frequency was 250 Hz in every weld. Experiments were carried out on a number of samples of 7025-T6. Three samples (*A*, *B* and *C*) had the same feed rate of 10 m/min so as to investigate the effect of heat input on the welds. The other three samples (*D*, *E* and *F*) had approximately the same heat input of 0.16 J/mm to investigate the effect of welding speed.

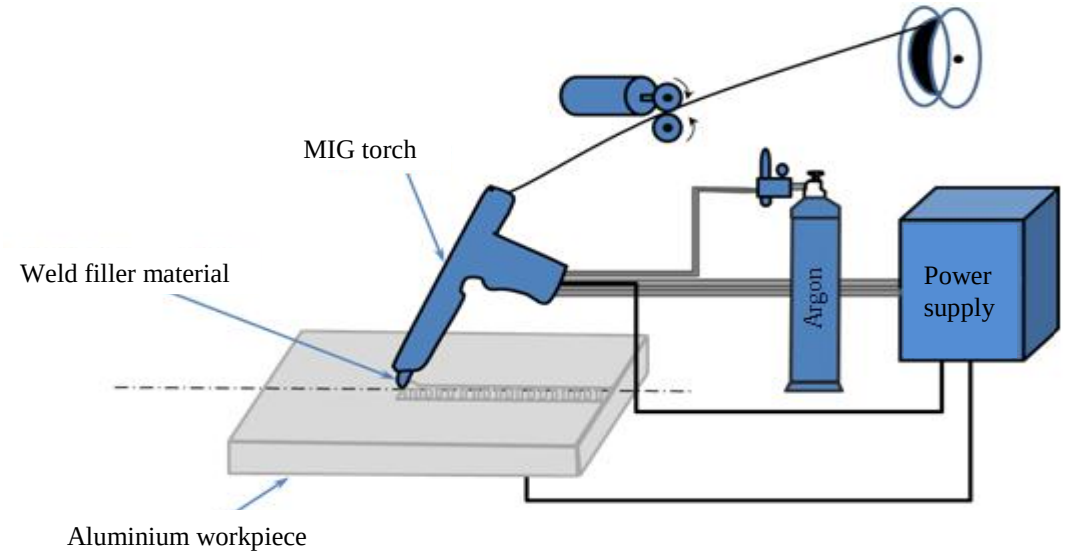

Fig. 1 Schematic diagram of experiment setup

3.3. Effect of welding heat input

In every fusion welding processes, there is the need for heat input; the heat is used to melt the aluminium (workpiece) to a fusible level so that it can be joined. The heat input level determines how fast the material melts and thus determines the maximum attainable welding speed. On the other hand, heat input can cause distortion, yielding poor weld quality. Therefore, there is a need to optimize the heat input. Furthermore, increase of heat energy incurs costs; reducing heat input and consequently energy consumption can help increase the economic efficiency of welding. In aluminium welding, the heat input must be controlled effectively due to aluminium's low melting point and high heat conductivity. The amount of heat input affects the macro and microstructure of the weld zone and thus the mechanical properties of the weld. As stated earlier, the pulsed MIG process allows for good heat input optimization.

Heat input has an effect on joint geometry, which includes weld penetration and weld width. With low heat input, the weld penetration is usually incomplete. As the heat input increases, the penetration increases and the weld appearance becomes better. However, the heat input also increases the size of the top side of the weld by widening the bead. The bottom widths of welds become larger with

high heat input. The width difference between the bottom and the top become smaller as the heat input increases, which may be due to the fact that the cooling rate decreases as the heat input increases (when the heat input is higher, more volume of the base metal will melt and the welding heat has more time to conduct into the bottom from the top) [7]. The base metal experience heat input that can be expressed qualitatively by the equation [8]:

$$Q = \frac{V\,I}{1000\,S}\,0.8\,. \qquad \text{(for MIG).} \qquad (1)$$

In Eq. (1), Q is heat input, $\eta = 0.8$ is the thermal efficiency, V is the arc voltage, I represent the current in amperes, and S represents the welding speed (mm/min). Heat input (kJ/mm) is given as the product of the voltage and thermal efficiency. This value changes depending on the type of shielding gas used, the shape and type of the electrode, and polarity. The constant, 0.8 accounts for the welding efficiency of the pulsed MIG process. Electromagnetic force is generated in the weld pool due to the strong current applied to generate the welding arc [8].

For samples *A-C* the wire feed rate was constant at 10 m/min and the heat input varied. For samples *D-F*, the heat input was approximately constant (0.16 kJ/mm) and the feed rates were selected as 10, 12 and 14 m/min respectively. A detrimental feature commonly found in aluminium processing is weakening of the metal due to heat input. The strength and other properties of the aluminium deteriorate thereby demanding remediation measures in subsequent processing. In aluminium welding, a weakening appears around the heat affected zone, known as HAZ softening. For example, in 6XXX series, the welding heat can reduce the strength of the parent metal by half. With 7XXX series, the weakening is of lesser severity but it extends even out from the weld [4].

Depending on the composition of the parent metal and the filler material used in the weld, the metal in the HAZ may be stronger or weaker than the parent metal. It is therefore important that welds should be located in regions of low stresses. HAZ softening though not exactly quantifiable without resorting to destructive testing, can be estimated to a certain extent, and in some cases, post weld treatment has to be carried out to improve the properties of the welded metal [9, 10].

3.4. Macroscopic examination of the weld

Examination of the weld was carried out in accordance with Finnish Standards Association SFS EN 1321, destructive testing of welds in metallic materials. The process of macroscopic examination started with the cutting of sample welds into small test pieces. The cuts were made perpendicularly to the weld axis to reveal the weld profiles of each sample. These samples were further processed by labelling one surface with a punch and grinding the other surface on a p100 silicon carbide grinding paper. Water was applied during grinding for cooling and lubrication. The samples were then cleaned with water and whipped dry using a tissue paper. The samples were then placed in Keller's reagent so as to reveal the joint profile and cleaned with propanol, after which they were then dried with a hot blower. The finished samples were photographed using a camera connected to a microscopic device. The camera was also connected to a TV monitor that displayed the pictures on a larger scale. The TV display was in black and white but the actual picture is coloured. The pictures were retrieved from the memory card of the camera as JPEG and then printed for further measurements and analysis. An example of a macro picture is presented in Fig. 2, showing the weld penetration.

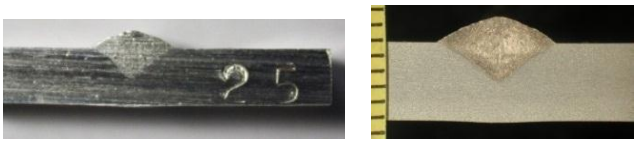

a b

Fig. 2 Weld samples a - non etched surface, b - etched surface by Keller's reagent

3.5. Hardness testing

Hardness testing of the welds was carried out based on the Vickers hardness test. The Vickers hardness test method involves indenting the test material with a diamond indenter in the form of a right pyramid with a square base and an angle of 136 degrees between opposite faces (Fig. 3) subjected to a weight of 1 to 100 kg. The full load is normally applied for 10 to 15 seconds. The two diagonals of the indentation made on the surface of the material after the removal of the load are measured using a microscope and their average calculated [11].

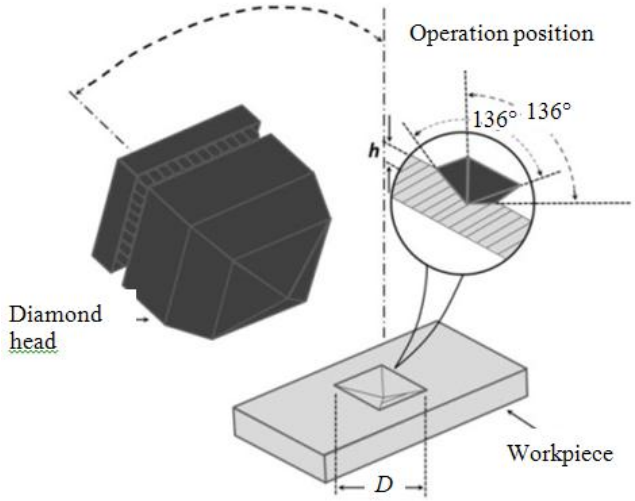

Fig. 3 Diamond pyramid indenter used for Vickers testing and resulting indentation in the workpiece. *D* is the mean diagonal of the indentation in mm

In this study the hardness test was carried out by indenting the diamond tool tip on the prepared weld cross section. A 3 kg weight was used for the indentation. The weight can be varied for different materials. In the case of aluminium, 3 kg is sufficient since aluminium is relatively soft. It should be noted that it is important that the weight is low enough for the aluminium test piece to be able to resist it. The indentations were done in rows at about 1 mm from the weld surface, as shown in Fig. 4.

The distance between each indentation is 0.7 mm and the indentations were rhombus-shaped. The principle

of the hardness test is that the depth of indentation depends on the hardness of the material. The dimension of the diagonals of an indentation was measured and the average value from the diagonals was found from the hardness table of HV3 to determine the hardness value. The values were then plotted against the distance of each indentation from the weld centre line.

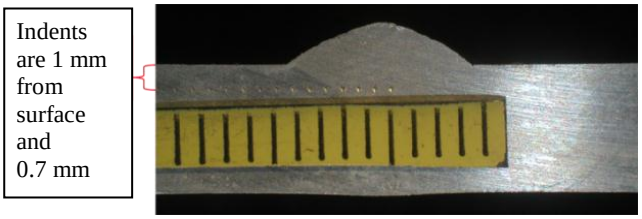

Fig. 4 Hardness testing of a weld sample

4. Results and discussions

The results of the experiment are based on microscopic and macroscopic examination of the workpiece and the hardness test of 7025-T6 aluminium alloys. The hardness tests of samples *A*-*C* are presented in Fig. 5, where the plots of *A*, *B* and *C* are combined on the same figure to allow for easier comparison. The weld interface (WI) is denoted by the vertical line labelled WI. The points on the graph curve indicate the distance of each indentation point from the weld centre line on the horizontal axis and the hardness value when traced to the vertical axis. The graph also shows the weld regions of unmixed zone (UZ) and partially melted zone (PMZ), the HAZ and the base material (BM). That is, sample *B* (0.127 kJ/mm) has about 120% heat input of sample *C* (0.106 kJ/mm) and sample *A* (0.318 kJ/mm) has 300% the heat input of sample *C* (Fig. 5).

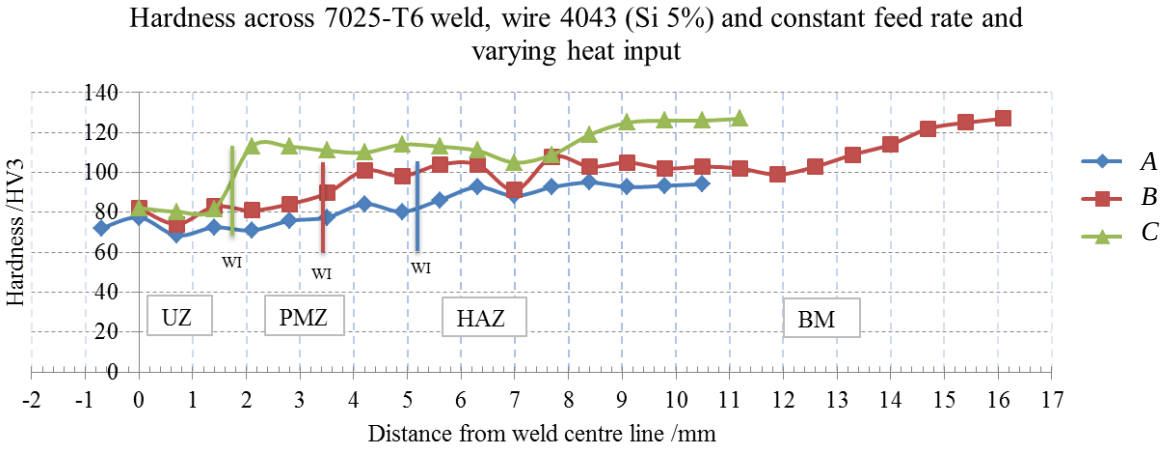

Fig. 5 Hardness testing of samples with varying heat input. *A* - 0.106 kJ/mm, *B* - 0.127 kJ/mm and *C* - 0.318 kJ/mm

When considering samples *A*, *B* and *C* for hardness, sample C has the greatest hardness (113 HV, just after the WI, about 2.1 mm away from weld centre line) followed by sample *B* and the least hardness value is found in sample *A*. This implies that the high heat input allows for high hardness of the WI, which is due to solution hardening during welding, i.e., high heat results in solutionizing, thereby causing higher hardening through the solidification process. It can also be said that the higher the heat input, the wider the weld bead and the further away from the weld centre line is the WI. Higher heat input also gives higher weld penetration. The hardness test of samples *D*, *E* and *F* is presented in Fig. 6. The heat input for the three samples is relatively constant. The labelling and description of the graph is the same as for samples *A*-*C*.

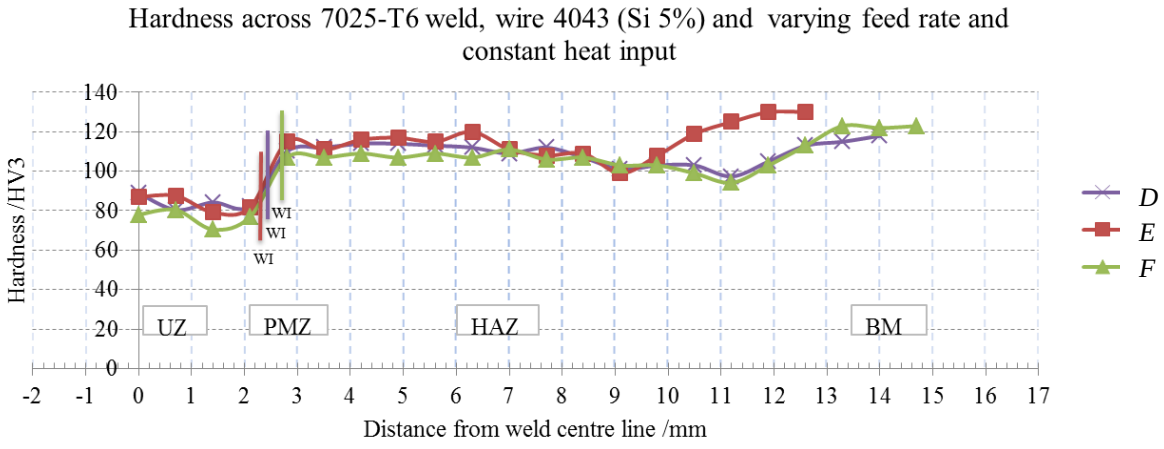

Fig. 6 Hardness testing of samples with relatively constant heat input of +/- 0,16 kJ/mm

The hardness pattern of samples *D*, *E* and *F* are similar but sample *E* has a small variation. The hardness around 3 mm away from the weld centre line shows a rapid increase in value from the previous point (around 2 mm from weld centre line). This is due to the closeness of the WI. From samples *D*, *E* and *F* it can be seen that for a 7025 weld, the hardness reduces in the weld zone and increases towards the base material. The hardness graph represents half of the symmetric welds. At the WI it can be said that the hardness value of *D*, *E* and *F* is relatively the same. This implies that at constant heat input, the hardness profile of 7025- T6 aluminium alloy remains the same.

The micro pictures of samples *A*-*F* are presented in Figs. 7-12, together with the parameters used for the welds. The picture of each sample shows the microstructure using an 8X magnification lens for the UZ, PMZ, HAZ and BM. The picture shows how the grains have been transformed, which is an indication of the properties of the weld of 7025 Al.

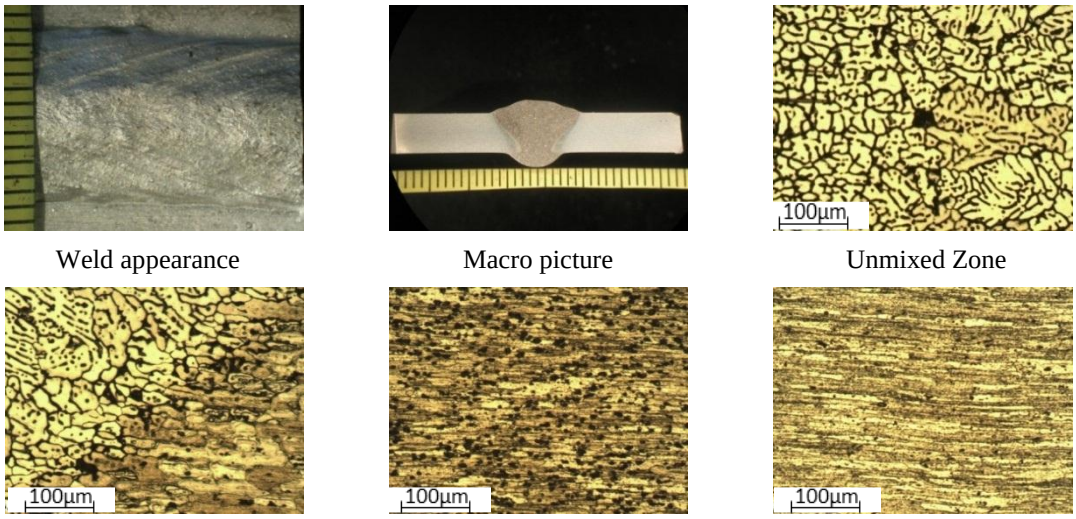

Weld appearance | Macro picture | Unmixed Zone

Partially Melted Zone | Heat Affected Zone | Base Metal

Fig. 7 Experimental results of sample *A* with feed rate (*FR*) of 10 m/min; welding speed (*S*) 10 mm/s; heat input *Q* = 0.318 J/mm; voltage *V* = 20.1 V; current *I* = 198 A

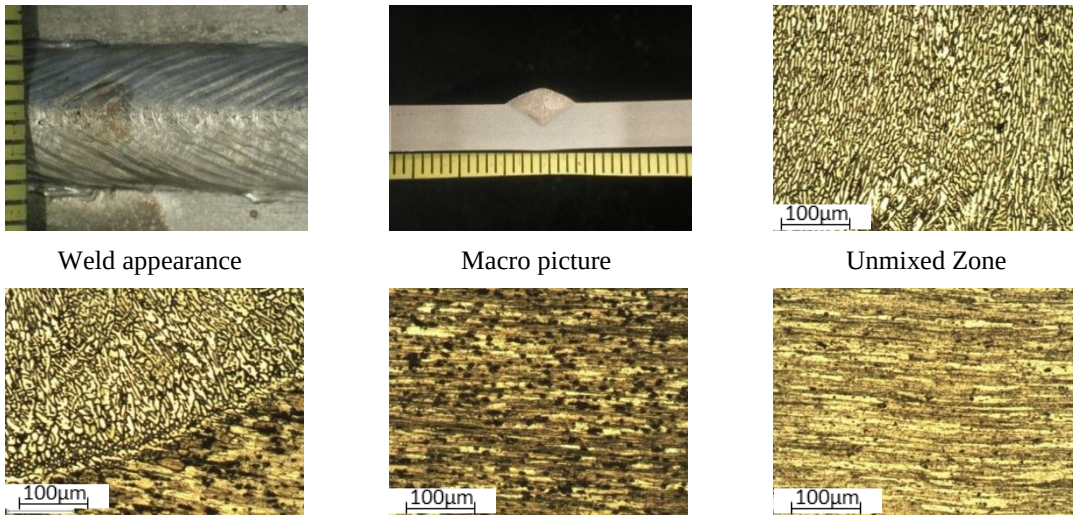

Weld appearance | Macro picture | Unmixed Zone

Partially Melted Zone | Heat Affected Zone | Base Metal

Fig. 8 Experimental results of sample *B* with feed rate *FR* = 10 m/min; *S* = 25 mm/s; *Q* = 0.127 J/mm; *V* = 19.4 V; *I* = 205 A

Comparing samples *A*, *B* and *C* in Fig. 7-9, it can be seen that the grain sizes around the WI are small when the heat input is low and vice versa. Furthermore, the transition flow of cells at the WI as it moves from the UZ to the HAZ is smoother with higher heat input where the grain sizes are bigger. With lower heat input, as in sample *C* (Fig. 9), the transition is not as smooth, so the WI is very distinct. The heat input is inversely related to the welding speed. When the welding speed increases, the heat input reduces. The higher the heat input, the higher the cooling rate. A high cooling rate allows for epitaxial growth and also for the cells to grow big, as seen by comparing sample *A* to sample *B* and *C*. In sample *A*, the HAZ is about 17 mm from the weld centre line, which is the greatest distance of the three samples (Fig. 7). Thus it can be said that the higher the heat input, the wider the HAZ.

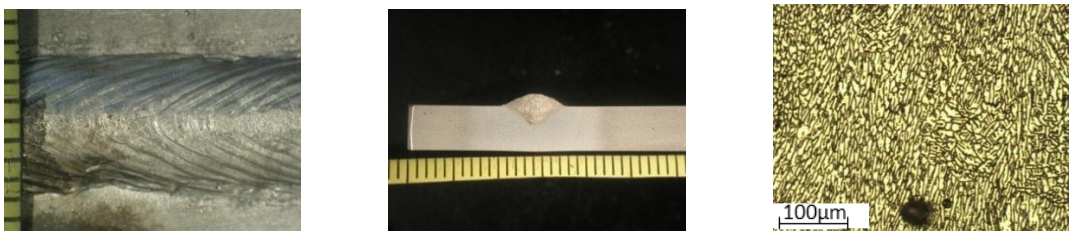

Weld appearance | Macro picture | Unmixed Zone

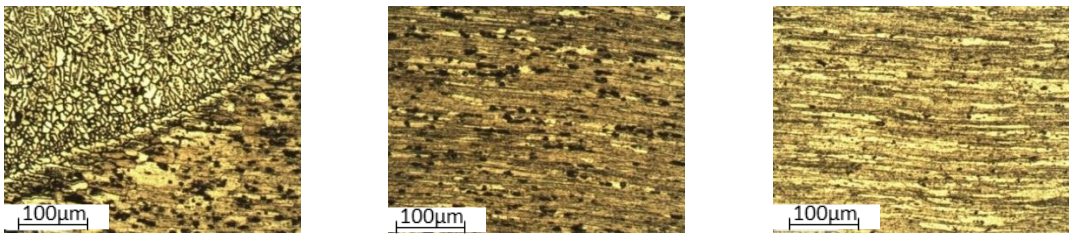

Partially Melted Zone | Heat Affected Zone | Base Metal

Fig. 9 Experimental results of sample *C* with feedrate *FR* = 10 m/min; *S* = 30 mm/s; *Q* = 0.106 J/mm; *V* = 19.4 V; *I* = 205A

The grains of UZ in sample *C* compared to *B* and *A* are very fine, which shows that the low heat input in samples *A* and *B* are insufficient to melt the pool and penetrate the weld. The high heat input and high welding speed caused high heat energy on the weld in sample *C*, which makes the weld bead large with a wider root.

Sample *C* has fine grains compared to *B* and *A*, which shows that with high heat input and welding speed, there is higher nucleation. In sample *C*, the grain growth is low compared to *A* and *B* because aluminium dissipates heat relatively fast through heat sinks; low heat input means that the effects of the high conductivity of aluminium strongly affect the weld microstructure (sample *C* cools fast).

By comparing the results of samples *D*, *E* and F as presented in Figs. 10-12, it can be noted that keeping the heat input relatively constant but varying the weld speed causes changes in the microstructure. As the welding speed increases and the feed rate is increased, the grain sizes increases. Furthermore, increased weld speed gives lower nucleation and coarser transitions of grains around the weld interface, which is similar to the effect of heat input in 7025 aluminium welds.

Samples *D*, *E* and *F* indicate that the higher the feed rate, the deeper the penetration. Sample *C* has a constant feed rate with *A* and *B* but the grain transition at the WI between the UZ and the HAZ is very sharp. This may be a possible failure point as the cells are not as interlocked as in sample *B*. Sample *A* shows that the longer the solidification time, the bigger the size of the dendrite [12].

The grains are equiaxed with dendrites within the grains. Fine grain sizes appear when the heat input is low and coarse grain sizes with high heat input. For example; the grain size in the unmixed zone of Fig. 9 has fine grains due to the low heat input of 0.106 kJ/mm while the unmixed zone of Fig. 7 has coarse grains in the unmixed zone due to the high heat input of 0.318 kJ/mm. The grain size variations in the unmixed zone of Figs. 7-12 is mainly due to the amount of heat input since high heat input means a high cooling rate.

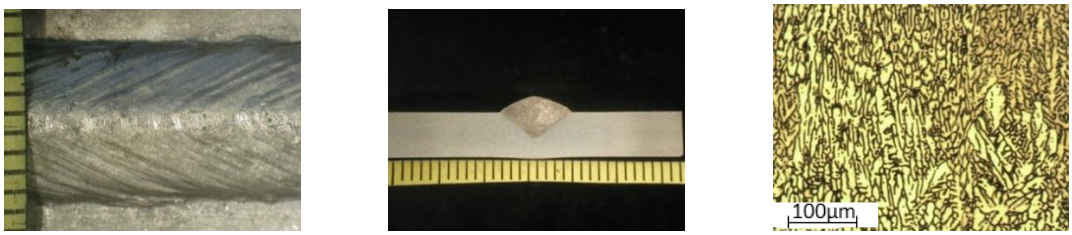

Weld appearance | Macro picture | Unmixed Zone

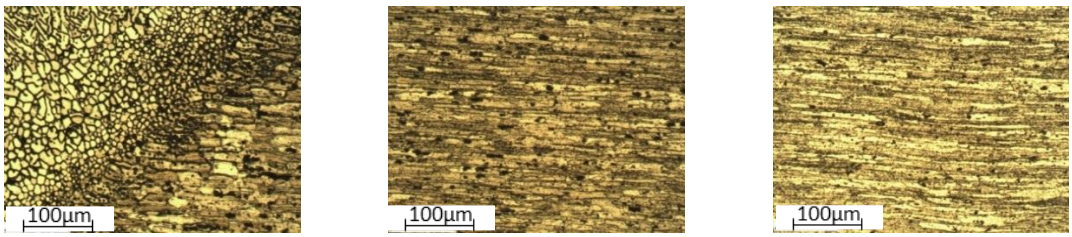

Partially Melted Zone | Heat Affected Zone | Base Metal

Fig. 10 Experimental results of sample *D* with *FR* = 10 m/min; *S* = 20 mm/s; *Q* = 0.16 J/mm; *V* = 19.8 V; *I* = 202 A

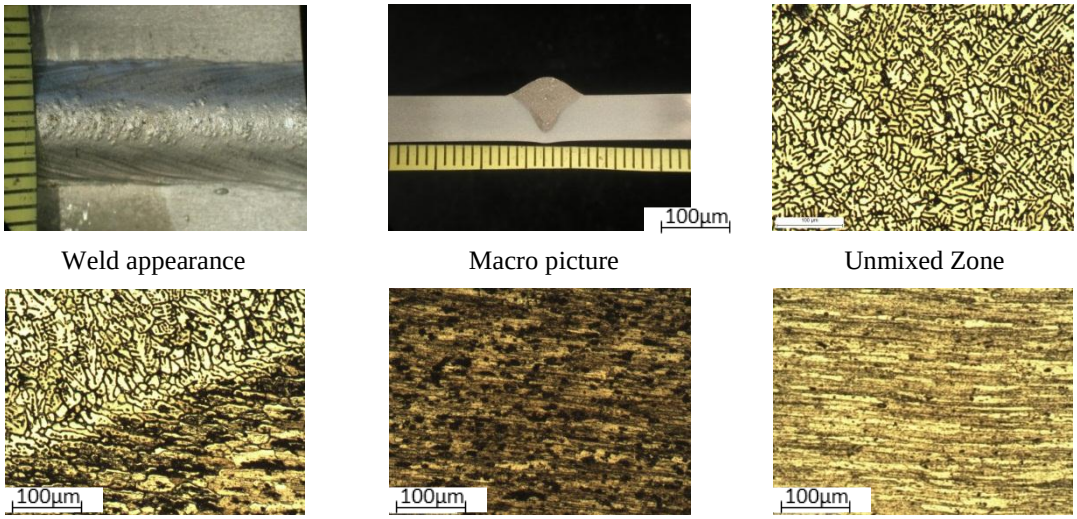

Weld appearance | Macro picture | Unmixed Zone

Partially Melted Zone | Heat Affected Zone | Base Metal

Fig. 11 Experimental results of sample *E* with *FR* = 12 m/min; *S* = 24 mm/s; *Q* = 0.163 J/mm; *V* = 20.30 V; *I* = 241 A

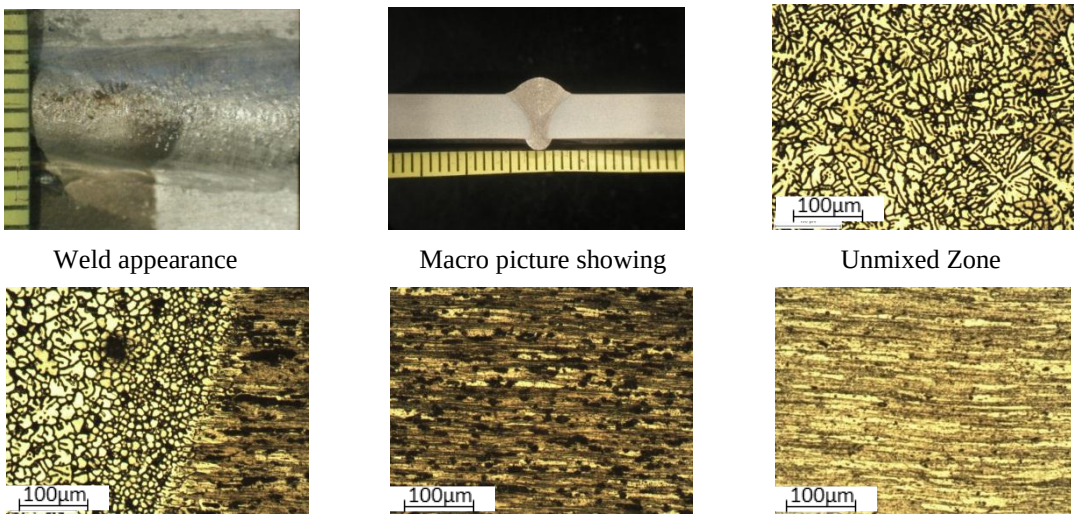

Weld appearance | Macro picture showing | Unmixed Zone

Partially Melted Zone | Heat Affected Zone | Base Metal

Fig. 12 Experimental results of sample *F* with *FR* = 14 m/min; *S* = 28.8 mm/s; *Q* = 0.158 J/mm; *V* = 20.50 V; *I* = 278 A

Faster welding speed allows for narrow seams even with lower heat input, seen by comparing samples *A*-*F*. Sample *F* seems to be the best weld with a narrow weld seam, narrow HAZ and complete penetration. On the other hand, oxidation occurred on the surface. At constant welding speed, high heat input increases the weld bead size and HAZ size. The PMZ shows epitaxial growth, which indicates that new grains had nucleated on the heterogeneous sites at the WI. There is a random orientation between the base metal grains and weld grains.

As can be seen from samples *A*-*F*, since the ratio of G/R decreases from the WI towards the centre line, the solidification modes have changed from planar to cellular, to columnar dendrite and equiaxed dendrite across the WI. The ratio of G/R determines the solidification modes found in the microstructure.

Sample *C* has the smallest grain size in the UZ. Thus it can be concluded that it has the highest strength and toughness as the Hall–Petch effect predicts that both strength and toughness increase as the grain sizes reduces. Sample *F* shows that complete weld penetration can be achieved with minimal heat input if other weld data are set correctly.

Minor weld defects such as porosity and oxidation are found on the welds. The porosity could be due to gas entrapment during the weld while the oxidation could be due to poor shielding gas covering (the weld pool has contact with atmospheric air).

5. Conclusions

1. In this study it has been seen that: with 7025-T6 aluminium alloys, the grain size reduces as the heat input reduces. The transition of cells from the UZ to HAZ is smoother with higher heat input. At constant heat input the coarse grain size increases in the HAZ when *FR*, *S* and *I* increase simultaneously but the hardness remains relatively constant.

2. When heat input is high, the HAZ is wider, the nucleation is lower, and the grains around the WI are coarser.

3. In the 7025 Al- alloy, high heat input allows for higher hardness of the weld interface due to the possibility of solution hardening. The higher the heat input, the wider the weld bead, the further away is the WI and the deeper the weld penetration.

4. The longer the solidification time, the bigger the size of the dendrites and a high cooling rate allows for epitaxial cell formation.

5. The 7025-T6 Al alloy, like other HAS alloys, experiences HAZ softening but can be restored by post-weld heat treatment.

References

1. **Graeve, I.D.; Hirsch, J.** 2010. 7xxx Series Alloys, aluminium.matter.org.uk/content/html/eng.
2. **Volpone, L.M.; Mueller**, **S**. 2008. Joints in light alloys today: the boundaries of possibility, Welding International 22(9): 597-609. http://dx.doi.org/10.1080/09507110802411518.
3. **Kah, P.; Hiltunen, E.; Martikainen, J.; Katajisto, J.** 2009. Experimental investigation of welding of aluminum alloys profiles and wrought plate by FSW, Mechanika 5(79): 21-27.
4. **Mathers, G.** 2002. The Welding of Aluminium and its Alloys, Woodhead Publishing, UK, 236p.
5. **George, E. T.; MacKenzie, D. S.** 2003. Handbook of Aluminium: Alloy Production and Materials Manufacturing. CRC Press, 736p.
6. **Boughton, P.; Matani, T.M.** 1967. Two years of pulsed arc welding, Welding and Metal Fabrication, October: 410-420.
7. **Mandal, N.R.** 2001. Aluminium Welding, Woodhead Publishing, 160p.
8. **Hirata, Y.** 2003. Pulsed arc welding, Welding International 17(2): 98-115. http://dx.doi.org/10.1533/wint.2003.3075.
9. **Kou, S.; Le, Y.** 1988. Welding parameters and the grain structure of weld metal - A thermodynamic consideration, Metallurgical and Materials Transactions A, 19(4): 1075-1082.
10. **Kah, P.; Salminen, A.; Martikainen**, **J**. 2010. The effect of the relative location of laser beam with arc in different hybrid welding processes, Mechanika 3(83): 68-74.
11. **ASM International; Chandler, H.** 1999. Hardness Testing, ASM International, 192p.
12. **Kou, S**. 2003. Welding Metallurgy, John-Wiley and Sons, 461p.

P. Kah, M. Olabode, E. Hiltunen, J. Martikainen

ALIUMINIO LYDINIO 7025 IMPULSINIS MIG SUVIRINIMAS

R e z i u m ė

Dėl elastingumo, lengvo svorio ir tamprumo aliuminio lydiniai plačiai naudojami pramonėje. Todėl svarbu tirti, kaip tokius lydinius kuo efektyviau suvirinti, nes, būdami gana lengvi, jie yra palyginti atsparūs. Šiame straipsnyje tiriamas impulsinis MIG (dujinis) labai atsparaus aliuminio (LAA) suvirinimas, atsižvelgiant į šilumos poveikio įtaką suvirinimo metalurgijai. LAA lydiniai dažniausiai naudojami aeronautikoje ir automobilių pramonėje, pvz., keleivinių vagonų konstrukcijose ir priekabų važiuoklėse.

Tiriamas impulsinis MIG lydinio 7025-T6 suvirinimas. Straipsnyje pateikiami robotizuotos impulsinės MIG suvirinimo mašinos eksperimentinių tyrimų rezultatai, gauti optinės mikroskopijos būdu vertinant suvirintos makro- ir mikrosiūlės struktūrą. Pateikiamos lydinio 7025-T6 mechaninių savybių (kietumo) pokyčių nuo šilumos poveikio priklausomybės. Suvirinimo šiluma veikia suvirinimo siūlės ir suvirinimo zonos kietumo kontūrą, kuris yra minkštesnis už bazinę medžiagą. Didinti šilumos poveikį aliuminiui 7025 leidžia tai, kad dėl mišinio sukietinimo suvirinimo vietoje didėja suvirinimo sujungimo kietumas.

P. Kah, M. Olabode, E. Hiltunen, J. Martikainen

WELDING OF A 7025 AL-ALLOY BY A PULSED MIG WELDING PROCESS

S u m m a r y

Aluminium alloys are important alloys in industries today, due to their ductile, lightweight and malleable nature. Research into how to effectively weld such alloys is therefore becoming increasingly important because of the considerable advantages of the material. Utilizing the high strength-to-weight ratio of aluminium alloys in welded products remains challenging but attainable. This paper studies pulsed MIG welding of a High Strength Aluminium (HSA) alloy, focusing specifically on the effect of heat input on the welding metallurgy. HSA alloys are used mostly in the aeronautic and automobile industries, e.g., in the construction of train coaches and trailer carriers.

Pulsed MIG welding of a 7025-T6 alloy is examined. The methodology for the paper is experimental investigation using a robotized pulsed MIG welding machine. Results are presented based on evaluation of the macrostructure and microstructure using optical microscopy. Mechanical properties (hardness variations) of 7025-T6 alloy welds with a range of heat inputs are also presented. Variations in the welding heat input affect the hardness profile, the weld seam and the weld zone, which is found to be soft compared to the base material. In 7025 aluminium, high heat input allows for higher hardness of the weld interface due to the possibility of solution hardening.

Keywords: high strength aluminium, hardness variation, 7025-T6 Al-alloy, 7XXX series, Pulsed MIG welding.

Received October 19, 2011
Accepted January 16, 2013